

## Zinc Mediates Assembly of the T1 Domain of the Voltage-gated K Channel 4.2\*

Received for publication, August 17, 2002, and in revised form, September 30, 2002  
Published, JBC Papers in Press, October 7, 2002, DOI 10.1074/jbc.M208416200

Alex W. Jahng<sup>‡§</sup>, Candace Strang<sup>¶</sup>, Don Kaiser<sup>‡||</sup>, Thomas Pollard<sup>‡\*\*</sup>, Paul Pfaffinger<sup>¶</sup>,  
and Senyon Choe<sup>‡ ‡‡</sup>

From the <sup>‡</sup>Structural Biology Laboratory, The Salk Institute, La Jolla, California 92037 and the <sup>¶</sup>Division of Neuroscience, S613, Baylor College of Medicine, 1 Baylor Plaza, Houston, Texas 77030

An intermolecular Zn<sup>2+</sup>-binding site was identified in the structure of the T1 domain of the Shaw-type potassium channels (αKv3.1). T1 is a BTB/POZ-type domain responsible for the ordered assembly of voltage-gated potassium channels and interactions with other macromolecules. In this structure, a Zn<sup>2+</sup> ion was found to be coordinated between each of the four assembly interfaces of the T1 tetramer by three Cys and one His encoded in the sequence motif (HX<sub>5</sub>CX<sub>20</sub>CC) of the T1 domain. This sequence motif is conserved among all non-Shaker-type voltage-dependent potassium (Kv) channels, but not in Shaker-type channels. The presence of this conserved Zn<sup>2+</sup>-binding site is a primary molecular determinant that distinguishes the tetrameric assembly of non-Shaker Kv channel subunits from that of Shaker channels. We report here that tetramerization of the *Shal* (rKv4.2) T1 in solution requires the presence of Zn<sup>2+</sup>, and the addition/removal of Zn<sup>2+</sup> reversibly switches the protein between a stable tetrameric or monomeric state. We further show that the conversion from tetramers to monomers is profoundly pH-dependent: as the solution pH gets lower, the dissociation rate increases significantly. The unfolding energy of the T1 tetramer as a measure of the conformational stability of the structure is also pH-dependent. Surprisingly, at a lower pH we observe a distinctly altered conformational state of the T1 tetramer trapped during the process of unfolding of the T1 tetramer in the presence of Zn<sup>2+</sup>. The conformational alteration may be responsible for increased rate of dissociation at lower pH by allowing Zn<sup>2+</sup> to be removed more effectively by EDTA. The ability of the T1 domain to adopt stable alternative conformations may be essential to its function as a protein-protein interaction/signaling domain to modulate the ion conduction properties of intact full-length Kv channels.

Voltage-gated, potassium ion selective (Kv) channels are found throughout most of the eukaryotic kingdom and display the widest range of channel properties among all voltage-gated ion channels (1–3). They are involved in various physiological functions such as the regulation of action potential firing and duration, endocrine and exocrine secretion, cardiac excitability,

learning and memory, as well as the control of synaptic efficacy. Functional Kv channels are formed by the tetramerization of their pore-forming α-subunits, a process regulated by the T1 domain of the channel (4, 5). Four major gene subfamilies (*Shaker* (Kv1), *Shab* (Kv2), *Shaw* (Kv3), and *Shal* (Kv4)) are designated by sequence similarity and their ability to homo- and heterotetramerize exclusively within subfamily members. In the crystal structures of *Shaker* (6) and *Shaw* T1 tetramers (7), four T1 subunits form a rotationally symmetric tetramer. The interfacial interaction is highly polar, and the interface residues show a high degree of sequence conservation within a subfamily, thus providing a structural explanation for the subfamily-specific assembly of Kv channels. Most recently, studies on the T1 domain as part of the intact channels have supported the idea that a tetrameric T1 domain with essentially similar atomic details to the crystallized structure is present within the full-length functional channel (8, 9).

The overall architecture of the T1 tetramer consists of four layer-like segments folded along the symmetry axis around the water-filled cavity termed the T1 cavity (see Fig. 1, layers 1–4 from the N terminus to the C terminus of the T1 chain, respectively). The T1 cavity, however, does not appear to be part of the ion permeation pathway (10), thus the cytoplasmic entryways for ions should lie between the T1 domain and the inner leaflet of the membrane, possibly forming four identical side openings through which ions can pass during ion conduction (8, 10–12). The C-terminal side of the T1 tetramer (layer 4) faces the inner leaflet of the membrane because the N-terminal side of the T1 tetramer (layer 1) interfaces the flat side of the Kvβ tetramer, making the N-terminal side most likely to face the cytoplasm (12). Zhou *et al.* (13) recently provided evidence to conclude that the N-terminal end of the unfolded polypeptide chain reaches the central pore cavity of the channel through this side opening. We have shown earlier that the putative membrane-facing side of T1 tetramer is conformationally flexible as compared with other parts of T1 (6, 10). Mutations within the T1 domain that alter the structure of the C-terminal side of the domain affect the gating properties of the channel, further arguing for a close association of this side of the domain with the transmembrane region (10, 14). A similar conformational change occurs within T1 tetramer when it is complexed with Kvβ tetramer (12).

The most striking difference between the Shaker channel T1 domain and the Shaw T1 domain is the presence of intersubunit-coordinated Zn<sup>2+</sup> ions in the assembly interface in Shaw channels. These Zn<sup>2+</sup> ions are coordinated by a C3H1 motif encoded within the conserved sequence (HX<sub>5</sub>CX<sub>20</sub>CC) of the T1 domain, located near the C-terminal end of the domain. This sequence is not found in any Shaker T1 domains but is highly conserved in *Shal*, *Shaw*, and *Shab* T1 domains, making it a

\* The costs of publication of this article were defrayed in part by the payment of page charges. This article must therefore be hereby marked "advertisement" in accordance with 18 U.S.C. Section 1734 solely to indicate this fact.

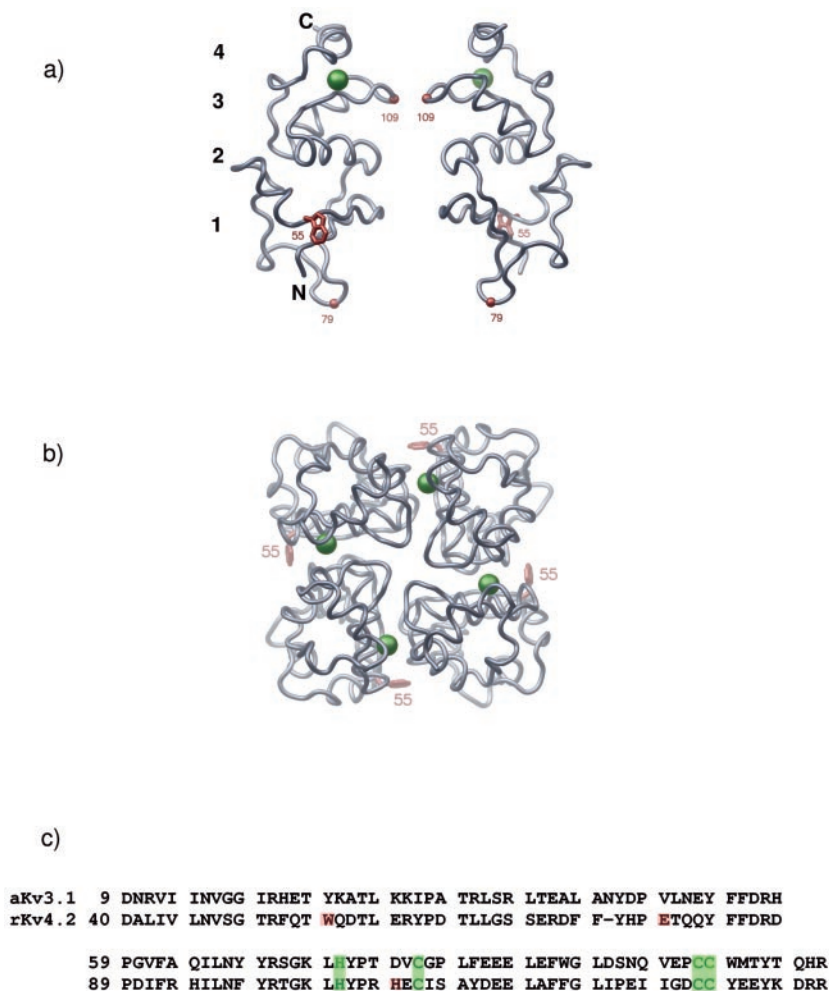
§ Present address: University of California, Irvine, CA 92697.

¶ Present address: The Burnham Inst., La Jolla, CA 92037.

\*\* Present address: Dept. of Molecular, Cellular, and Developmental Biology, Yale University, New Haven, CT 06520.

‡‡ To whom correspondence should be addressed. Fax: 858-452-3683; E-mail: choe@salk.edu.

**FIG. 1. Homology model of rKv4.2 T1 tetramer built on the published aKv3.1 T1 tetramer structure (7).** The model was created using the program O by a simple mutation method. *a*, side view of T1 tetramer. The 4-fold symmetry axis is vertical in this view. Only two subunits are shown for clarity. Numbers 1–4 on the left side denote layers 1 through 4 from the N terminus to the C terminus of the chain. *N* and *C* denote N and C terminus, respectively. *b*, cross-sectional view of T1 tetramer is shown from the C-terminal side of T1 tetramer. The green spheres are four Zn<sup>2+</sup> ions buried in the tetrameric interface. The Trp-55, the only Trp present within the T1 domain of the rKv4.2 is indicated in red. C $\alpha$  positions of Glu-79 and His-109 of rKv4.2 corresponding to positions of Kv $\beta$  contacting Leu-76 of rKv1.1 (12) and cavity-widening Asn-136 of aKv1 (10), respectively, are shown in red as a ball. *c*, amino acid sequence alignment between aKv3.1 (top) and rKv4.2 (bottom). Four Zn-coordinating amino acids are highlighted in green boxes. Trp-55, Glu-79, and His-109 of rKv4.2 are shown in red boxes.



characteristic difference between Shaker channels and all other Kv channels. These four amino acids are fully exposed on the subunit interface with one histidine and two cysteine residues from one subunit and a cysteine residue from the facing subunit. However, the locations of four Zn atoms within the tetramer are deeply buried inside the protein, ~6 or 14 Å from the exterior or interior of the protein surface of the tetramer, respectively (7). This location suggests that Zn<sup>2+</sup> may not directly interact with the channel gating or permeation machinery, but rather likely alters the properties of the T1 domain itself to explain its striking conservation in non-Shaker-type channels.

To elucidate the roles such Zn<sup>2+</sup> ions might play in the non-Shaker-type Kv channels, we have examined the biochemical roles of Zn<sup>2+</sup> in Shal T1 domain assembly and structural stability. In this report, we demonstrate that Zn<sup>2+</sup> is absolutely essential for the stable maintenance of Kv4.2 T1 tetramer in solution. We then show that removal and addition of Zn<sup>2+</sup> directly results in conversion between monomer and tetramer interchangeably. We further demonstrate that the conversion between tetramer and monomer is pH-dependent, and there is a distinctly altered conformation of T1 tetramer at slightly acidic pH. Such conformational plasticity can enable T1 to mediate signaling through various protein-protein interactions with the cytoplasmic components, such as with K channel-interacting proteins (KchIP) (15), or Src tyrosine kinases (16), and Kv $\beta$  (17), to regulate Kv channels. These results clearly support that a probable conformational linkage propagating through the T1 tetramer can act as a signaling mediator for protein-protein interactions (18), thus implicating T1 as an

essential structural platform for channel regulation through interactions with cytoplasmic proteins. Consistent with this idea, structural models to regulate conductance of bacterial channels through conformational changes of cytoplasmic domains have been recently reported (19, 20).

#### MATERIALS AND METHODS

**Protein Preparation**—A modified pET20b vector carrying the His-tagged version of rKv4.2 T1 domain (residues 41–161) were transformed into BL21(DE3) P-LysS cells. Cells were grown at 37 °C in the LB medium containing 100  $\mu$ g/ml ampicillin and 34  $\mu$ g/ml chloramphenicol and were induced with 1 mM IPTG<sup>1</sup> at 22 °C for 4–5 h when the A<sub>600</sub> reached 1–2.0. The cells were pelleted and then sonicated in buffer containing 20 mM Tris, pH 8.0, 300 mM NaCl, 5 mM  $\beta$ -ME, and 50  $\mu$ M ZnSO<sub>4</sub>. The soluble fraction was collected for nickel-nitrilotriacetic acid/His-tag purification (Qiagen). For the preparation of apo-protein, the purified T1 sample was dialyzed for over 36 h in the Tris buffer containing 2 mM EDTA. The tetrameric and monomeric forms were then separated through a fast protein liquid chromatography S75 column (Amersham Biosciences) in their buffers containing either 50  $\mu$ M ZnSO<sub>4</sub> or 2 mM EDTA, respectively, for further experiments. MES was used to buffer for pH values 6.0 and 6.5, HEPES for pH values 7.0 and 7.5, Tris for pH values 8.0 and 8.5, and 3-[1,1-dimethyl-hydroxyethyl)-amino]-2-hydroxypropanesulfonic acid (AMPSO) for pH 9.0 and 9.5. The protein was stored at 4 °C until use.

**Analytical Centrifugation**—1 mg/ml of protein was loaded on to Beckman Optima-XLA in Tris, pH 8.0, buffer containing either 2 mM EDTA or 50  $\mu$ M ZnSO<sub>4</sub>. The protein was run at three different speeds overnight. The data were analyzed by the program Origin (adapted for the Optima XLA by Beckman, Palo Alto, CA).

<sup>1</sup> The abbreviations used are: IPTG, isopropyl-1-thio- $\beta$ -D-galactopyranoside; MES, 4-morpholineethanesulfonic acid.

**Intrinsic Fluorescence Measurements**—All the fluorescence measurements were done on a fluorimeter (Photon Technology International). The excitation/emission monochrome slit widths were 1 nm. The excitation wavelength was 283 nm for both the wavelength scans and the time-based scans. The emission wavelength was at 339 nm, and the average value was obtained over 10 s.

**Kinetics of Association and Dissociation**—Monomerization of T1 tetramer was initiated by incubating 50  $\mu\text{g}$  of protein in the 1 ml of buffer containing 2 mM EDTA. Tetramerization of T1 monomer was initiated by incubating 50  $\mu\text{g}$  of protein in 1 ml of buffer containing  $\text{ZnSO}_4$  in 200  $\mu\text{M}$  excess of 2 mM EDTA. Monomerization experiments were initiated manually with the dead time of up to 4 s, with the exception of the reaction carried out at pH 6.0, which was carried out using a manual stopped-flow instrument. All the tetramerization experiments were carried out on the manual stopped-flow instrument. Fluorescence intensity was measured over time to follow the reactions. Each data point is an average of 3–6 measurements. The increase in fluorescence intensity is linearly proportional to the concentration of tetramer ([T]) and the remaining to be [M] by subtracting [T] from the constant starting concentration. The resulting data were fit to an equation with a single exponential to derive the rate,  $k$  in the unit of  $\text{sec}^{-1}$ , in which  $[\text{M}] = k_{\text{m}} [\text{T}]$  and  $[\text{T}] = k_{\text{t}} [\text{M}]$ , respectively.

**Equilibrium Denaturation**—A 50- $\mu\text{g}$  protein sample was dissolved in 1 ml of the corresponding denaturation buffer that ranged in urea concentration from 0 to 7.6 M and was equilibrated at room temperature for 2–6 h before measurement. The extent of denaturation was assayed by change in intrinsic fluorescence. The corresponding denaturation data were fit to the equation for the empirical two-state denaturation states by the program Kaleidograph.

## RESULTS

**Tetramerization of Shal T1 Domain Critically Depends on the Presence of  $\text{Zn}^{2+}$** —The first question that we sought to answer was whether the interfacial  $\text{Zn}^{2+}$  ions present in the T1 domain are important for subunit tetramerization. To address this question we assessed the molecular size and stability of the isolated rKv4.2 T1 domain in the presence of either  $\text{Zn}^{2+}$  or the  $\text{Zn}^{2+}$  chelator EDTA, by size-exclusion chromatography and sedimentation equilibrium centrifugation. The protein is first prepared as a pure tetramer by nickel-nitrilotriacetic acid affinity column chromatography from a soluble cytoplasmic fraction of *Escherichia coli* lysate. Protein samples were dialyzed against the chromatography buffer (20 mM Tris, pH 8.0, 300 mM NaCl, and 5 mM  $\beta$ -mercaptoethanol) containing either 50  $\mu\text{M}$   $\text{Zn}^{2+}$  or 2 mM EDTA overnight prior to a size-exclusion chromatography. By atomic absorption, the proteins incubated in  $\text{Zn}^{2+}$  contain 1 ion of  $\text{Zn}^{2+}$  per T1 molecule, whereas those incubated in EDTA contain essentially 0 ions of  $\text{Zn}^{2+}$  per T1 molecule. These results were not affected by the His<sub>6</sub> tag because identical measurements are made with or without the His tag removed by proteolytic digestion.

T1 samples elute from the fast protein liquid chromatography size exclusion chromatography column Superdex 75 at 64.5 and 85.4 min in  $\text{Zn}^{2+}$  or EDTA, respectively (Fig. 2). These are the estimated elution time for Stokes' radii of tetrameric and monomeric T1, respectively, based on the elution times for other protein standards. No other size protein peak was detected in these experiments, suggesting that the T1 domain has only 2 stable quarternary states, monomer or tetramer. These results are reproduced for samples prepared at pH values 6.5, 7.0, 7.5, 8.5, 9.0, and 9.5. Without addition of  $\text{Zn}^{2+}$  or EDTA to the buffer, the T1 sample is very stable as a tetramer, which contains a stoichiometric amount of  $\text{Zn}^{2+}$  (one per subunit) as measured by atomic absorption. In this case the  $\text{Zn}^{2+}$  ions were probably picked up from the *E. coli* culture media during protein expression and retained within the structure by high affinity binding. As further evidence of the high affinity  $\text{Zn}^{2+}$  binding, EDTA is essential to dissociate T1 tetramer into monomers because dialysis against a buffer without  $\text{Zn}^{2+}$  for up to 3 days does not measurably dissociate tetramers. T1 monomers in EDTA solution were indefinitely stable at concentrations as

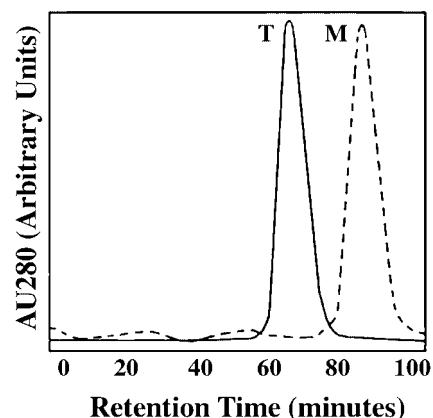


FIG. 2. Elution profile of the rKv4.2 T1 domain in Superdex75, run at 1 ml/min. The sample elutes at 64.5 min in the presence of 50  $\mu\text{M}$   $\text{Zn}^{2+}$  at pH 8.0 (solid line) and at 85.4 min in the presence of 2 mM EDTA (dotted line). The calculated molecular masses in the presence of  $\text{Zn}^{2+}$  and EDTA are 74.2 kDa and 13.1 kDa, respectively. The elution time of the molecular mass standards are 53.4 min for  $\beta$ -amylase (200 kDa), 56.9 min for alcohol dehydrogenase (150 kDa), 63.1 min for bovine serum albumin (66 kDa), 76.9 min for carbonic anhydrase (29 kDa), and 86.0 min for cytochrome C (12.4 kDa).

high as 10 mg/ml within our experimental timeframe (days). We used uniformly 2 mM EDTA in this study, which has an expected binding constant of  $10^{-15}$  M for free  $\text{Zn}^{2+}$  in solution.

Molecular weight estimates of proteins based on Stokes' hydrodynamic size of the molecule as measured by the elution times from sizing chromatography columns can be affected by molecular shape and possible interaction between the sample and the gel matrix. Therefore, sedimentation equilibrium experiments at three different speeds were also carried out to obtain a shape-independent accurate measurement of the molecular weights of the species in the same buffers with either  $\text{Zn}^{2+}$  or EDTA. The data were fit with the assumption that there are only two species (monomer or tetramer) present in each of the two conditions (Fig. 3). The molecular mass estimate of the molecule in the presence of  $\text{Zn}^{2+}$  is 62.0 kDa, whereas it is 16.5 kDa in the presence of EDTA, respectively. These measurements agree very well with the calculated molecular mass of Kv4.2 T1 tetramers (61.6 kDa) and monomers (15.4 kDa). The excellent fit under the two-species model also suggests that there are no other stable oligomeric states such as dimers or trimers in detectable amounts.

**Monomerization and Tetramerization Rates are pH-Dependent**—The sequence of the rKv4.2 T1 contains a single Tryptophan at position 55 (highlighted in Fig. 1). This Trp side chain is positioned near the surface-exposed exterior of the T1 tetramer at the interfacial junction between adjacent subunits and thus is likely to change in environment as the protein changes from monomer to tetramer. We therefore used this Trp as a spectroscopic probe to measure the conformational changes of the protein under different conditions. We first measured differences in the Trp fluorescence for T1 tetramers or monomers prepared as described above for size exclusion chromatography. The tetramers were excited at 283 nm, and their emission maximum was measured at 339 nm (Fig. 4). The Trp fluorescence intensity of the tetramer at 339 nm is, however, about twice that of the monomer, which has the maximum emission wavelength red-shifted to 343 nm. We could therefore use this large difference in emission to follow the kinetics of T1 domain assembly or disassembly upon  $\text{Zn}^{2+}$  addition or chelation. Based on the empirical two-states monomer-tetramer model, the resulting data were fit with a single exponent to derive the conversion rates:  $k_{\text{m}}$  from tetramer to monomer and  $k_{\text{t}}$  from monomer to tetramer. Assembly of mono-

FIG. 3. Distributions of the concentrations of rKv4.2 T1 domain in the presence of  $50 \mu\text{M}$   $\text{Zn}^{2+}$  (a) or  $2 \text{ mM}$  EDTA (b), analyzed by the analytical centrifugation run at 14, 20, and 28 K rpm. The pH of both samples is 8.0. The derived molecular masses of the species are 62.0 kDa and 16.5 kDa, respectively. The lines through the data points were calculated with either tetramer or monomer, respectively, to show excellent fits with little deviation, validating the conclusion that there are only two species (either monomer or tetramer) in each sample.

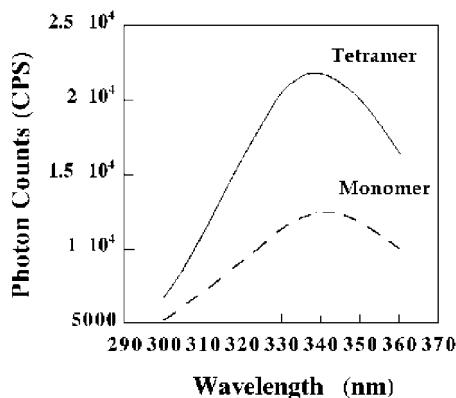


FIG. 4. Steady-state fluorescence of the T1 tetramer in  $50 \mu\text{M}$   $\text{Zn}^{2+}$  buffer (a) and T1 monomer in  $2 \text{ mM}$  EDTA buffer (b) both at pH 8.0. Excitation wavelength was 283 nm with 1 nm excitation/emission monochrome slit. The emission maximum for the T1 tetramers is 339 nm; the emission maximum for the T1 monomers is 343 nm.

mers to tetramer was initiated by adding  $2.2 \text{ mM}$  of  $\text{Zn}^{2+}$  ( $200 \mu\text{M}$  in excess over EDTA) to  $50 \mu\text{g/ml}$  of monomers. In the standard buffer condition at pH 7.5, the rate of T1 tetramerization,  $k_t$ , is  $\sim 0.14$  per second. To measure the disassembly rate,  $k_m$ , conversion of tetramers to monomers was initiated by incubating  $50 \mu\text{g/ml}$  of tetramer ( $\sim 1 \mu\text{M}$  monomer concentration) with  $2 \text{ mM}$  EDTA. The disassembly rate under these conditions was  $\sim 0.01$  per second.

There was no significant change in the shape and magnitude of the monomer or tetramer emission spectra at different pH levels, but the rate of conversion between the tetramer and monomer is highly pH-dependent. At lower pH, the  $\text{Zn}^{2+}$ -coordinating ligands (imidazole group on His and sulfhydryl group on Cys) will be titrated with protons making them less favorable for binding  $\text{Zn}^{2+}$ . As expected, the tetramerization ( $k_t$ ) rate increases slightly as the pH becomes more basic, consistent with the notion that deprotonation would favor metal binding (Fig. 5). The tetramerization rate could not be accurately measured at pH 9 or higher because  $\text{Zn}^{2+}$  precipitates at such basic pH levels, probably as a complex with hydroxides. The monomerization ( $k_m$ ) rate, however, showed a much greater pH dependence in rate between pH 6.0 and 9.0, compared with a relatively insignificant difference in  $k_t$  over the same pH range. Indeed, at pH 6.0, the monomerization rate becomes  $\sim 10$ -fold faster than tetramerization. Measurements below pH 6.0 could not be made because the T1 protein precipitates appreciably at such acidic pH levels.

If the  $\text{Zn}^{2+}$ -binding sites were freely accessible in solution, the rate dependence on pH for tetramerization and monomerization would be reciprocally related as dictated by the free energy change associated with pH (protonation) state. Our results indicate therefore that the physical access to  $\text{Zn}^{2+}$  by

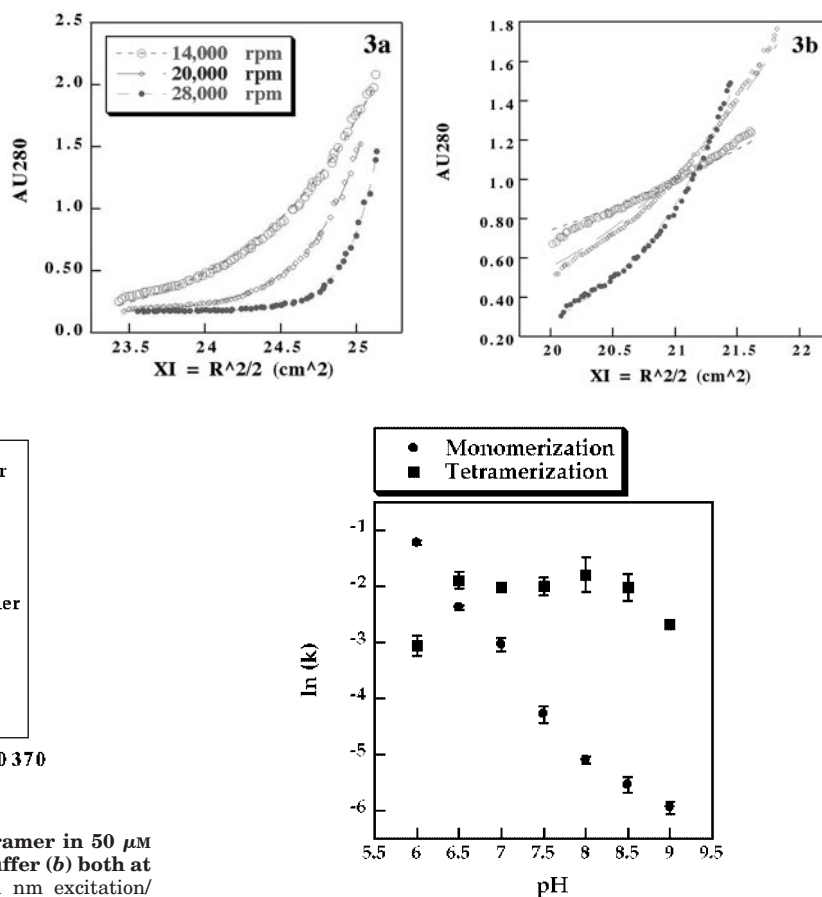


FIG. 5. Natural log plots of the rates ( $k$ ) of self-association of the monomers ( $k_t$ , solid squares) and dissociation of the tetramers ( $k_m$ , solid circles) plotted against pH. Each data point is an average of 3–6 measurements. Rates are in the unit of  $\text{sec}^{-1}$  to relate the concentrations of monomers and tetramer in the first-order kinetic terms.

EDTA is a time-limiting step, which requires partial disassembly of the T1 tetramer. For such a “buried”  $\text{Zn}^{2+}$ , the effects of solution pH or local ionic strength on the rates of disassembly will primarily reflect properties of conformational dynamics of the protein structure rather than on  $\text{Zn}^{2+}$ -EDTA affinity alone. We conclude therefore that the profound dependence of  $k_m$  on pH reflects limited accessibility of EDTA to the  $\text{Zn}^{2+}$ -binding sites buried within the protein, which become more accessible at acidic pH.

*An Altered Conformation of Kv4.2 T1 Tetramer Is Detectable during the Process of Partial Denaturation of the Protein*—If the conformational dynamics of the T1 tetramer are pH-dependent, as predicted above, then lower pH should also affect the free energy profile of the unfolding process for the T1 tetramer carried out in the presence of  $50 \mu\text{M}$   $\text{Zn}^{2+}$ . We used the fractional change in Trp fluorescence emission as a function of urea concentration to measure the amount of the unfolded protein to detect any changes in the thermodynamic stability of the protein fold, as measured by linear extrapolation to  $0 \text{ M}$  denaturant (25). At pH levels more acidic than 7.5, the denaturation midpoint shift progressively to the left (lower urea concentration), but the slope of transition near the mid-point of denaturation does not change (Fig. 6). An altered slope would have been indicative of the changes in cooperativity among four subunits during the unfolding process. Thus, these results are consistent with the conclusion that the T1 tetramer interface does not associate cooperatively to influence the rate of dissociation of the T1 tetramer as a function of pH, instead the

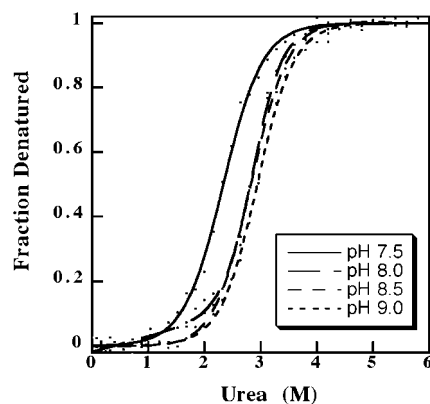


FIG. 6. Unfolding curves for the T1 tetramers at four pH levels: 7.5, 8.0, 8.5, and 9.0. Protein samples were fully equilibrated in a standard buffer with  $50 \mu\text{M}$   $\text{Zn}^{2+}$ . Fractions of unfolding are derived from changes in the fluorescence intensity.

conformational flexibility of the protein itself increases at lower pH.

In contrast, at pH 7.0 we found that the denaturation curve is shaped in the form of two S curves, with a more sensitive change in Trp emission evident in the region below 2.5 M urea followed by second change in Trp emission above 3.0 M urea (Fig. 7). Changes in the conformational energy profile by pH may indicate the existence of alternate conformations of the T1 tetramer, to which the equilibrium may shift at lower pH. Analytical centrifugation or gel filtration chromatography of the T1 domain in 2.5 M urea with  $\text{Zn}^{2+}$  reveals that all the protein is still tetrameric, indicating that this change in Trp emission is produced within the tetrameric T1 domain. The simplest explanation for these results is that at acidic pH an altered conformation is readily accessible in which the single Trp residue is exposed to a more aqueous environment thus changes the fluorescence emission. The transition midpoint to the intermediate conformer is  $\sim 0.8$  M urea, at pH 7.0, indicating a small energy difference to the standard T1 tetramer conformation at this pH. Based on our observation of the essential role of  $\text{Zn}^{2+}$  for tetramerization and the increased rate of monomerization at lower pH, we conclude that the faster dissociation of the T1 tetramer at lower pH is facilitated by the presence of an altered conformation that T1 tetramer can adopt at lower pH.

#### DISCUSSION

The existence of  $\text{Zn}^{2+}$  at the assembly interface as originally visualized in the crystal structure of Shaw-type Kv channel T1 domain (7) raised the question of what the role of  $\text{Zn}^{2+}$  is in the channel protein. In this study, we have used size-exclusion chromatography, analytical centrifugation, and fluorescence spectroscopy as tools to study the role of  $\text{Zn}^{2+}$  in the conversion of T1 domain between monomer and tetramer and to follow the process of protein unfolding through urea denaturation. We have shown that removal of  $\text{Zn}^{2+}$  from the T1 tetramer by EDTA is energetically sufficient to break apart the T1 tetramer into stable monomers, although the rate of conversion is limited by the inaccessibility to the buried  $\text{Zn}^{2+}$  within the protein. Addition of  $\text{Zn}^{2+}$  to the T1 monomer rapidly and reversibly reassembles the domain into a tetramer, indicating that the monomer is a stable folded state of the protein that can exist without the presence of  $\text{Zn}^{2+}$ .

Fluorescence intensity at 339 nm reports primarily an environmental change around the single Trp-55 that is predicted to contribute to the subunit tetramerization interface (see Fig. 1B). The increased intensity and the slight blue shift upon T1 tetramerization indicates that the single Trp, with probably a

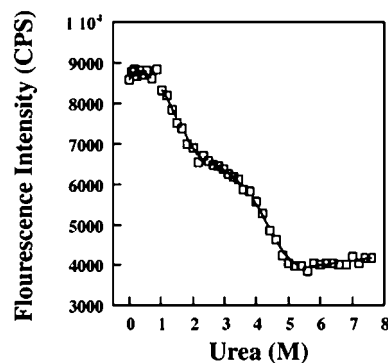


FIG. 7. The profile of denaturation at pH 7 is shown directly by the raw fluorescence intensity change as a function of urea concentration. The data were obtained during the denaturation of the T1 tetramers at pH 7.0 in the presence of  $\text{Zn}^{2+}$ . The unfolding pathway is no longer sigmoidal and displays a three-states denaturation pathway.

small fraction of the signal contributed by the 10 Tyr residues present in the T1 domain, moves toward a hydrophobic environment within the subunit interface of the T1 tetramer. By characterizing the molecular sizes of the T1 domain under the same solution conditions, we confirm that this change in fluorescence emission spectra is produced by protein monomerization. During the conversion to the partially or fully disassembled conformation, the T1 domain likely retains the same tertiary structure intact upon release of  $\text{Zn}^{2+}$  because the conversion is fully reversible, and the fluorescence intensity is further reduced upon complete unfolding by the addition of 8 M urea to the monomers. In this context, the presence of water-stable monomers is strikingly interesting to us, although it is not completely surprising based on the fact that the interface consists of highly polar amino acids (6, 7).

The exact role of  $\text{Zn}^{2+}$  for intact Kv channels are far from being understood completely. The work described in this paper clearly shows that  $\text{Zn}^{2+}$  binding provides sufficient energy for the tetramerization of the isolated Kv4.2 T1 domain. Furthermore, we show that the kinetic rate of disassembly to monomers is highly pH-dependent, primarily by the putative conformational alterations induced by lower pH so that the  $\text{Zn}^{2+}$  can be more readily removed. This conclusion is supported by our unexpected observation that a stable intermediate conformation presumably trapped in a local energy minimum is detected at slightly acidic pH after a partial denaturation by urea. It remains to be understood whether pH and  $\text{Zn}^{2+}$  interact under physiological conditions to modulate the tetrameric assembly of non-Shaker-type Kv channels. Mutations introduced to the  $\text{Zn}^{2+}$ -coordinating side chains of Kv4.2 channel subunits cause inefficient formation into functional channels in the membrane, but intact channels do not respond to Zn chelators added into the cytoplasm<sup>2</sup>. These results confirm the essential roles of  $\text{Zn}^{2+}$  for the stability and rigidity of the functional channels. Channels show more complex responses to acid treatment.

A large change in the ability of the T1 domain to access this alternative conformation at pH 7.0 or below suggests that the T1 domain may act as a pH sensor under physiological conditions. Local protonation can alter the structure of the domain and potentially the stability of protein-protein interactions or channel gating properties. However, there is no evidence whether this conformational flexibility is present to endow pH-sensing ability to the domain. Nevertheless, the conformational flexibility of T1 tetramer induced by solution pH sug-

<sup>2</sup> C. Strang, K. Kanjilwar, D. Debruis, D. Peterson, and P. Pfaffinger, manuscript in preparation.

gests a plausible mechanism by which binding of cytoplasmic proteins to the T1 tetramer can trigger a conformational change through the protonation of a specific set of amino acids locally. Such conformational alteration and its propagation through T1 tetramer can be a general mechanism by which protein-protein interactions in the cytoplasm affect channel functions, for which we demonstrate  $Zn^{2+}$  plays an indirect but essential structural role.

Our future studies are aimed at determining what roles  $Zn^{2+}$  and the T1 domain play in defining the electrophysiological and regulatory properties of the channel itself. Despite varying degrees of emphasis on the importance and role of the N-terminal cytoplasmic domain in the regulation of channel properties (8, 10, 21–24), it becomes evident that conformational changes in the cytoplasmic domains play a direct role in regulating the transmembrane pore regions of the channel (10–12, 19, 20). Apparently, an ion channel in the cell membrane is not an isolated independent protein but rather a complex assemblage of multiple structural and regulatory proteins, the full extent of which is only recently emerging (26). The location of the T1 domain at the heart of such a multi-protein complex suggests that understanding the intricacies and roles of this domain requires complete knowledge on the context under which it naturally resides.

## REFERENCES

- Hille, B. (1992) *Ionic Channels of Excitable Membranes*, Sinauer Associates, Sunderland, MA
- Jan, L. Y., and Jan, Y. N. (1990) *Trends Neurosci.* **13**, 415–419
- Salkoff, L., Baker, K., Butler, A., Covarrubias, M., Pak, M. D., and Wei, A. (1992) *Trends Neurosci.* **15**, 161–166
- Li, M., Jan, Y. N., and Jan, L. Y. (1992) *Science* **257**, 1225–1230
- Shen, N. V., and Pfaffinger, P. J. (1995) *Neuron* **14**, 625–633
- Kreusch, A., Pfaffinger, P. J., Stevens, C. F., and Choe, S. (1998) *Nature* **392**, 945–948
- Bixby, K. A., Nanao, M. H., Shen, N. V., Kreusch, A., Bellamy, H., Pfaffinger, P. J., and Choe, S. (1999) *Nat. Struct. Biol.* **1**, 38–43
- Kobertz, W. R., Williams, C., and Miller, C. (2000) *Biochemistry* **39**, 10347–10352
- Strang C., Cushman, S. J., DeRubeis, D., Peterson, D., and Pfaffinger, P. J. (2001) *J. Biol. Chem.* **276**, 28493–28502
- Cushman, S., Manao, M. H., Jahng, A. W., DeRubeis, D., Choe, S., and Pfaffinger, P. J. (2000) *Nat. Struct. Biol.* **7**, 403–407
- Choe, S., Kreusch, A., and Pfaffinger P. J. (1999) *Trends Biol. Sci.* **24**, 345–349
- Gulbis, J., Zhou, M., Mann, S., and MacKinnon, R. (2000) *Science* **289**, 123–127
- Zhou, M., Morais-Cabral, J. H., Mann, S., and MacKinnon, R. (2001) *Nature* **411**, 657–661
- Minor, D. L., Lin, Y. F., Mobley, B. C., Avelar, A., Jan, Y. N., Jan, L. Y., and Berger, J. M. (2000) *Cell* **102**, 657–670
- An, W. F., Bowlby, M. R., Betty, M., Cao, J. Ling, H. P., Mendoza, G., Hinson, J. W., Mattsson, K. L., Strassle, B. W., Trimmer, J. S., and Rhodes, K. J. (2000) *Nature* **403**, 553–556
- Holmes, T. C., Fadool, D. A., Ren, R., and Levitan, I. B. (1996) *Science* **274**, 2089–2093
- Rettig, J., Heinemann, S. H., Wunder, F., Lorra, C., Parcej, D. N., Dolly, J. O., and Pongs, O. (1994) *Nature* **369**, 289–294
- Lockless, S. W., and Ranganathan, R. (1999) *Science* **286**, 295–299
- Roosild, T., Miller, S., Booth, I., and Choe, S. (2002) *Cell* **14**, 781–791
- Jiang, Y., Lee, A., Chen, J., Cadene, M., Chait, B. T., and MacKinnon, R. (2002) *Nature* **417**, 515–522
- Lee, T. E., Philipson, L. H., Kuznetsov, A., and Nelson, D. J. (1994) *Biophys. J.* **68**, 664–673
- van Dongen, A. M. J., Frech, G. C., Drewe, J. A., Joho, R. H., and Brown, A. M. (1990) *Neuron* **5**, 433–443
- Tu, L., Santarelli, V., Sheng, Z., Skach, W., Pain, D., and Deutsch, C. (1996) *J. Biol. Chem.* **271**, 18904–18911
- Zerangue, N., Jan, Y. N., and Jan, L. Y. (2000) *Proc. Natl. Acad. Sci. U. S. A.* **97**, 3591–3595
- Bolen, D. W., and Santoro, M. M. (1988) *Biochemistry* **27**, 8069–8074
- Hisi, H., Ward, M. A., Choudhary, J. S., Blackstock, W. P., and Grant, S. G. N. (2002) *Nat. Neurosci.* **3**, 661–669